Longitudinal distribution of chlorine absorption in human airways: a comparison to ozone absorption

Vladislav Nodelman and James S. Ultman

J Appl Physiol 87:2073-2080, 1999.

Longitudinal distribution of chlorine absorption in human airways: a comparison to ozone absorption

VLADISLAV NODELMAN AND JAMES S. ULTMAN
Biomolecular Transport Dynamics Laboratory, Department of Chemical Engineering, Pennsylvania State University, University Park, Pennsylvania 16802

Nodelman, Vladislav, and James S. Ultman. Longitudinal distribution of chlorine absorption in human airways: a comparison to ozone absorption. *J. Appl. Physiol.* 87(6): 2073–2080, 1999.—The bolus inhalation method was used to measure the fraction of inhaled chlorine (Cl_2) and ozone (O_3) absorbed during a single breath as a function of longitudinal position in the respiratory system of 10 healthy nonsmokers during oral and nasal breathing at respired flows of 150, 250, and 1,000 ml/s. At all experimental conditions, <5% of inspired Cl_2 penetrated beyond the upper airways and none reached the respiratory air spaces. On the other hand, larger penetrations of O_3 beyond the upper airways occurred as flow increased and during nasal than during oral breathing. In the extreme case of oral breathing at 1,000 ml/s, 35% of inhaled O_3 penetrated beyond the upper airways and ~10% reached the respiratory air spaces. Mass transfer theory indicated that the diffusion resistance of the tissue phase was negligible for Cl_2 but important for O_3. The gas phase resistances were the same for Cl_2 and O_3 and were directly correlated with the volume of the nose and mouth during nasal and oral breathing, respectively.

air pollution; inhalation toxicology; lung dosimetry; mass transfer coefficient; regional uptake

CHLORINE (Cl_2) and ozone (O_3) are gaseous pollutants that can irritate the human respiratory tract. The time-weighted exposure limit of Cl_2 and O_3 exposure for an 8-h work shift are 0.5 and 0.1 parts per million (ppm) by volume, respectively (1). Short-term exposure of volunteers to Cl_2 concentrations as low as 1.0 ppm and O_3 concentrations as low as 0.12 ppm can cause decrements in forced vital capacity and forced expiratory volume in 1 s (11, 14). Although the health effects of long-term Cl_2 and O_3 exposure in humans have not been determined, nonneoplastic lesions have been observed in animals chronically exposed to O_3 or Cl_2. In rats and monkeys, airway lesions resulting from Cl_2 exposure were focused primarily in the nasal cavities (10, 16), whereas lesions resulting from O_3 exposure were observed in alveolated air spaces (2, 4). It is possible that these differences in lesion distribution were due to corresponding differences between the uptake patterns of Cl_2 and O_3.

The uptake of O_3 has been determined by direct sampling of respired gas within the human respiratory tract (5, 6). These experiments made use of indwelling tubes that limited measurements to only a few large airway sites and undoubtedly disturbed local flow and concentration profiles. To circumvent these problems, the distribution of O_3 uptake in the human respiratory tract can be noninvasively measured by bolus inhalation, an indirect method that utilizes gas sampling at the airway opening alone (7). Bolus inhalation measurements indicated that the portion of inhaled O_3 absorbed in the upper airways of healthy adult nonsmokers is 80% during quiet nasal breathing compared with 50% during quiet oral breathing. In neither case did O_3 reach the respiratory air spaces (9). When oral flow was increased to a light exercise condition of 1,000 ml/s, however, 25% of inhaled O_3 reached the respiratory air spaces (8). Recently, the bolus inhalation method was adapted to Cl_2. During nasal and oral quiet breathing, >90% of inhaled Cl_2 was absorbed in the upper airways of healthy nonsmokers (12).

In the present work the longitudinal distributions of Cl_2 and O_3 were directly compared in the same group of healthy nonsmokers during nasal and oral breathing at respiratory flows of 150, 250, and 1,000 ml/s. Because O_3 is a poorly soluble gas whereas Cl_2 rapidly and reversibly hydrolyzes in aqueous solution, it is hypothesized that increasing the respiratory flow will increase the amount of O_3 but not Cl_2 that reaches the respiratory air spaces during either mode of breathing. The availability of uptake data from these two gases of widely different solubilities also provides an opportunity to study the relative role of their gas phase and mucus phase diffusion resistances. Although a bolus inhalation study of O_3 uptake during oral breathing at 150–1,000 ml/s has been carried out (8), it was important to repeat these experiments on the same group of subjects and with the identical breathing apparatus used to obtain the Cl_2 bolus inhalation data.

MATHEMATICAL MODELING

As previously described by Nodelman and Ultman (12), the human airways were modeled as a series of nasal/oral (N/O), pharyngeal (PH), lower airway (LA), and respiratory air space (RA) compartments. On the basis of a simplified solution of the one-dimensional unsteady diffusion equation, Hu and associates (8) derived the relationship between the absorbed fraction (Λ) and the penetration volume (V_P) of a reactive gas bolus inhaled into such a compartmental model. For ease in applying a linear regression analysis, this relationship can be expressed as follows

$$\ln(1-\Lambda) = -(2/\dot{V})\{(Ka)_{N/O}(V_{PO}-V_P) + I_1[(Ka)_{PH}-(Ka)_{N/O}](V_{PI}-V_P) + I_2[(Ka)_{LA}-(Ka)_{PH}](V_{P2}-V_P)\} \quad (1)$$

The costs of publication of this article were defrayed in part by the payment of page charges. The article must therefore be hereby marked "*advertisement*" in accordance with 18 U.S.C. Section 1734 solely to indicate this fact.

where $\dot{V}$ is the respiratory flow rate and $(Ka)_i$ is the product of an overall mass transfer coefficient (K) and the surface-to-volume ratio (a) in *compartment i* (i.e., N/O, PH, or LA). V_{P0}, V_{P1}, and V_{P2} are the penetration volumes that correspond to the entrance of the N/O, PH, and LA compartments, respectively. I_1 and I_2 are indicator variables defined as follows: $I_1 = 1$ if $V_P > V_{P1}$, and $I_1 = 0$ otherwise; $I_2 = 1$ if $V_P > V_{P2}$, and $I_2 = 0$ otherwise. The RA compartment has been omitted from *Eq. 1*, because the reactive gas reaching this compartment was never sufficient to allow a reliable estimation of $(Ka)_{RA}$.

The local absorption of Cl_2 and O_3 can be better understood by considering the individual factors that contribute to Ka. As Cl_2 or O_3 absorbs into an airway (or air space), it encounters a diffusion resistance created by a respiratory gas boundary layer and a second resistance imposed by the surrounding mucus (or surfactant) film. The overall resistance to mass transfer within a compartment is equal to the sum of these diffusion resistances (15)

$$1/Ka = 1/k_g a + \lambda/k_{ti} a \quad (2)$$

where k_g and k_{ti} are the individual mass transfer coefficients in the gas boundary layer and the mucus layer, respectively, and λ is the equilibrium partition coefficient of Cl_2 or O_3 concentration between gas and mucus. Of particular importance is the fact that k_g depends on the geometry and gas flow in the airway lumen.

The value of k_g in a specific geometry is often predicted from equations of the following form (15)

$$Sh = m' Re^n Sc^p \quad (3)$$

where m', n, and p are constants. As applied to radial absorption of Cl_2 or O_3 in an airway, the Sherwood (Sh), Reynolds (Re), and Schmidt (Sc) numbers are dimensionless groups defined by

$$Sh \equiv k_g d/D_g,\ Re \equiv \dot{V} d/A\nu,\ Sc \equiv \nu/D_g \quad (4)$$

where d is the airway diameter, A is the cross section available for flow, D_g is the binary diffusivity of Cl_2 or O_3 in air, and ν is the kinematic gas viscosity. Combining *Eqs. 3* and *4* results in

$$k_g = m\dot{V}^n d^{n-1}/A^n \quad (5)$$

where

$$m = m' D_g^{1-p} \nu^{p-n} \quad (6)$$

The value of ν can be approximated by the viscosity of pure air, $(D_g)_{Cl_2}/(D_g)_{O_3}$ is estimated to be 0.8 (15), and $p = 0.8$–1.3 in human airways (13). It follows from *Eq. 6* that m has similar values for Cl_2 and O_3 and from *Eq. 5* that k_g is essentially the same for the two gases. In addition, the average value of n for inspiration and expiration is close to unity (13), so *Eq. 5* may be approximated as

$$(k_g a/\dot{V}) = (ma/A) \quad (7)$$

where m can be considered to be a constant, whereas a and A depend on compartment geometry.

Because $k_g a/\dot{V}$ is essentially the same for both test gases, *Eq. 2* can be simultaneously applied to Cl_2 and O_3

$$1/Ka = (\dot{V}/k_g a)(1/\dot{V}) + (\lambda/k_{ti} a)_{Cl_2} I + (\lambda/k_{ti} a)_{O_3}(1 - I) \quad (8)$$

where $I = 1$ when Ka corresponds to Cl_2 absorption and $I = 0$ when Ka refers to O_3 absorption. Within a particular airway compartment of a particular subject, *Eq. 7* implies that $k_g a/V$ is constant, and *Eq. 8* further implies that plots of $1/Ka$ vs. $1/\dot{V}$ for Cl_2 and for O_3 should be parallel lines with a common slope of $\dot{V}/k_g a$ but different intercepts of $(\lambda/k_{ti} a)_{Cl_2}$ and $(\lambda/k_{ti} a)_{O_3}$, respectively.

METHODS

Subject population. Five healthy men and five healthy nonpregnant women, all nonsmokers with no history of cardiovascular, pulmonary, and upper airway disease or allergy, were accepted in the investigation. For each subject, nasal volume (V_{NS}) and cross-sectional area (A_{NS}), oral volume (V_{OR}) and cross-sectional area (A_{OR}), and pharyngeal volume (V_{PH}) and cross-sectional area (A_{PH}) were measured by acoustic reflection. Conducting airway volume (V_D) was determined by single-breath nitrogen washout during oral breathing. Lower conducting airway volume (V_{LA}) was defined as $V_D - (V_{OR} + V_{PH})$. The subjects in this study were the same as those in a study of Cl_2 uptake during quiet breathing, for which more detailed descriptions of the screening procedures and the respiratory system volume measurements were previously reported (12). All procedures employed in the present experiments, including the informed consent of each subject, were approved by the Institutional Review Board of the Pennsylvania State University.

Bolus measurements. The bolus inhalation apparatus consisted of a custom-designed Teflon breathing assembly that monitored respiratory flow and Cl_2 and O_3 concentration and injected boluses containing a peak pollutant concentration of 3.0 ppm Cl_2 or 1.0 ppm O_3. A mouthpiece or a nasal cannula fixture could be attached to the proximal end of the breathing assembly for oral or nasal breathing maneuvers, respectively. The volume of both fixtures was 20 ml. The detailed design and performance of the bolus inhalation system were described previously (12). The only modification of the apparatus made in this study was the use of a larger heated pneumotachometer (model 4719, Hans Rudolph) to monitor respired flow in the 1,000 ml/s experiments than was used in the previous quiet breathing experiments.

During a research session, the subject was seated comfortably on a stool, wore noseclips during oral breathing, and maintained a closed mouth during nasal breathing. To carry out a bolus test breath, the subject donned the mouthpiece or nasal cannula, activated the inhalation apparatus by depressing a hand-held switch, and inhaled beginning at functional residual capacity while viewing a computer monitor on which the integrated pneumotachometer signal (i.e., the respired volume) was displayed in real time. Throughout the breath, the subject corrected his or her respiratory flow rate so that respired volume coincided, as closely as possible, with a predrawn isosceles triangle corresponding to equal inspiratory and expiratory flows of 150, 250, or 1,000 ml/s and an inhaled tidal volume of 500 ml. At a predetermined time during inhalation, a Cl_2-air or O_3-air bolus was automatically injected into the inspiratory flow. Because the subject always

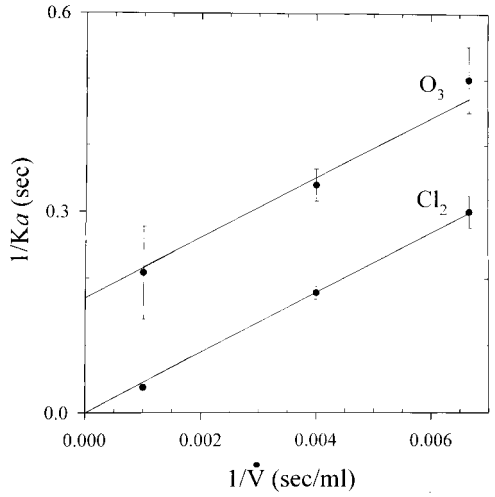

Fig. 1. Representative $(1/Ka)$-$(1/\dot{V})$ regression, where K is mass transfer coefficient, a is surface-to-volume ratio, and $\dot{V}$ is respiratory flow rate. Data points and vertical bars represent means ± SE of $1/Ka$ in oral (OR) compartment of an individual subject. According to *Eq. 8*, intercept of O_3 line is $(\lambda/k_{ti}a)_{O_3}$, intercept of Cl_2 line is $(\lambda/k_{ti}a)_{Cl_2}$, and common slope of 2 lines is $(\dot{V}/k_g a)$, where λ is equilibrium partition coefficient and k_g and k_{ti} are mass transfer coefficients in gas boundary and mucus layers, respectively.

began a test breath at functional residual capacity, the penetration of the bolus into the respiratory system could be systematically varied from breath to breath by changing the injection time. A complete experiment consisted of 50–70 bolus test breaths recorded at penetrations of 0–200 ml.

All 10 subjects participated in six sessions lasting 2–4 h, in which Cl_2 or O_3 bolus measurements were made during nasal and oral breathing at a fixed respired flow of 150, 250, or 1,000 ml/s. For each subject, a Cl_2 session at 250 ml/s was carried out first. This was followed by Cl_2 sessions at 150 and 1,000 ml/s that were performed in an order that was randomized among subjects. The same sessions were then repeated using O_3 as a test gas. Within each session, the order of nasal and oral experiments was randomized, and bolus test breaths were carried out at increasing penetrations in some experiments but at decreasing penetrations in other experiments. To minimize carryover of exposure effects, each session was separated by ≥1 wk.

Data analysis. As previously described in detail (12), the Cl_2 and O_3 concentration curves of each bolus test breath were numerically integrated with respect to respired volume to determine Λ (the amount of pollutant absorbed during a single respiratory cycle relative to the inhaled amount) and V_P (the mean airway volume that would be reached by inhaled Cl_2 or O_3 molecules relative to the gas sampling point if no absorption occurred). To estimate compartmental values of the overall mass transfer parameter (Ka), a splined linear least-squares regression of *Eq. 1* to each subject's Λ-V_P test breath data was separately performed at each respiratory flow, for nasal and oral breathing, and for Cl_2 or O_3 absorption.

Values of $\dot{V}/k_g a$, $(\lambda/k_{ti}a)_{Cl_2}$, and $(\lambda/k_{ti}a)_{O_3}$ were estimated within the N/O and PH compartments of each subject by regression of *Eq. 8* to the Ka values for Cl_2 and O_3 at the 150, 250, and 1,000 ml/s respired flows. Regression was performed with a nonlinear weighted least-squares Marquart algorithm (Sigma-Plot, SPSS) in which $\dot{V}/k_g a$, $(\lambda/k_{ti}a)_{Cl_2}$, and $(\lambda/k_{ti}a)_{O_3}$ were treated as adjustable parameters, and the weights were inversely proportional to the standard errors of the subject's Ka estimates (Fig. 1). The LA compartment was excluded from this analysis because of extensive absorption of Cl_2 in the more proximal compartments.

To calculate the fraction of inhaled Cl_2 or O_3 that was absorbed within each of the five compartments ($\Delta\Lambda$), the Λ values of Cl_2 or O_3 at the proximal boundaries of the PH, LA, and RA compartments were first calculated from *Eq. 1*. $\Delta\Lambda$ within a compartment was then calculated as the difference between the Λ values of Cl_2 or O_3 at the distal and proximal boundaries of the compartment.

A two-tailed Student's *t*-test was used to compare parameter values between different experimental conditions. Comparisons were made only if at least eight values were available at each condition. Paired comparisons were made when values for all 10 subjects were available in both compared conditions. Otherwise, an unpaired comparison was made. The risk of making a type I error in the comparisons was controlled at $\alpha = 0.05$.

RESULTS

Characteristics of subjects. The anthropometric characteristics of the 10 healthy, young, adult nonsmokers who participated in the study are given elsewhere (12), and their compartmental volumes and average cross-sectional areas are given in Table 1. Whereas V_{NS} was somewhat smaller than V_{OR} ($P = 0.18$) for the subject population as a whole, there was no correlation between V_{NS} and V_{OR} [coefficient of determination adjusted for number of subjects (r^2) = 0.00]. The values of V_{OR} and A_{OR} for different subjects were highly correlated ($r^2 = 0.85$), the values of V_{PH} and A_{PH} were reasonably correlated ($r^2 = 0.50$), but the values of V_{NS} and A_{NS} were not correlated ($r^2 = 0.00$).

Absorbed fraction. In Fig. 2 the Λ-V_P distributions are pooled for all participants at each experimental condition. On average, Cl_2 was absorbed more efficiently than O_3 during nasal and oral breathing. Furthermore, the difference between the absorption efficiency of Cl_2 and O_3 increased with increasing respiratory flow rate during nasal and oral breathing. For example, during nasal breathing at a respiratory flow rate of 150 ml/s, values of Λ at the proximal end of the pharynx in an average subject (i.e., V_P = 64 ml)

Table 1. *Compartmental dimensions of the study population*

	V_{OR}, ml	V_{NS}, ml	V_{PH}, ml	V_{LA}, ml	A_{OR}, cm²	A_{NS}, cm²	A_{PH}, cm²
Mean ± SD	54 ± 20	44 ± 4	22 ± 10	78 ± 26	5.3 ± 1.7	2.4 ± 0.4	2.4 ± 0.9
Range	22–80	37–51	8–37	41–114	2.7–8.2	1.9–3.2	1.2–4.0

V_{OR}, combined volume of oral cavity and oropharynx (OR); V_{NS}, combined volume of nasal cavities and nasopharynx (NS); V_{PH}, volume of hypopharynx (PH); V_{LA}, volume of lower conducting airways ($V_D - V_{OR} - V_{PH}$; LA); A_{OR}, average cross-sectional area (i.e., ratio of volume to length) of OR compartment; A_{NS}, average cross-sectional area of NS compartment; A_{PH}, average cross-sectional area of PH compartment.

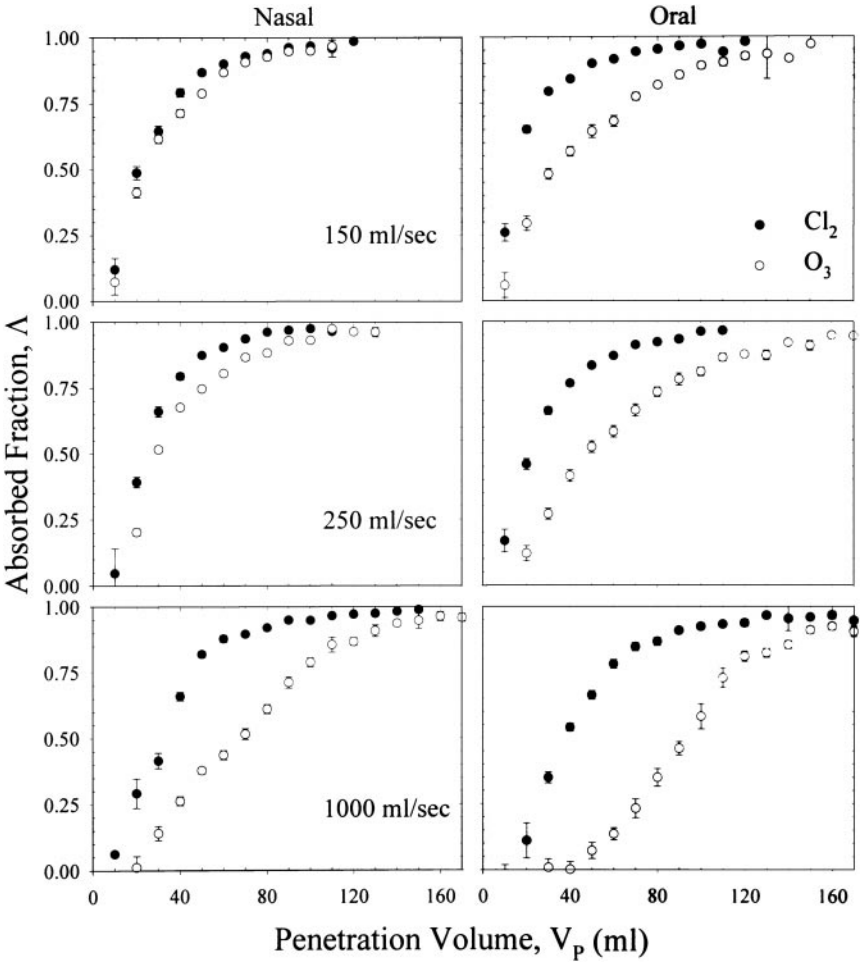

Fig. 2. Λ-V_P distributions pooled for 10 subjects. Data points and vertical bars represent means ± SE of absorbed fraction (Λ) within 10-ml increments of penetration volume (V_P). SE includes between- and within-subject variations. Peak inspired Cl_2 concentration was 3.0 parts per million (ppm), and peak inspired O_3 concentration was 1.0 ppm.

were ~0.95 for Cl_2 and 0.90 for O_3. When the respiratory flow was increased to 1,000 ml/s, Λ decreased to 0.90 for Cl_2 and 0.45 for O_3. Similarly, during oral breathing at 150 ml/s, the values of Λ at the proximal end of the pharynx in an average subject (i.e., V_P = 74 ml) were 0.95 for Cl_2 and 0.80 for O_3, but Λ decreased to 0.85 for Cl_2 and 0.25 for O_3 when the respiratory flow increased to 1,000 ml/s.

Figure 2 also indicates that Cl_2 absorption was similar during nasal and oral breathing but O_3 absorption was more efficient during nasal breathing, particularly at the higher respiratory flows. For example, Λ for Cl_2 at the proximal boundary of the pharynx was 0.95 during nasal and oral breathing at 150 ml/s and 0.90 during nasal breathing and 0.85 during oral breathing at 1,000 ml/s. In contrast, the corresponding values of Λ for O_3 were 0.90 during nasal breathing and 0.80 during oral breathing at 150 ml/s and 0.45 during nasal breathing and 0.25 during oral breathing at 1,000 ml/s. As a result, a higher dose of inspired O_3 was absorbed in the PH, LA, and RA compartments during oral breathing than during nasal breathing.

$\Delta\Lambda$ of Cl_2 and O_3 in each of the four airway compartments is shown in Fig. 3. Relative to O_3, the dose distribution of Cl_2 exhibits a much weaker dependence on respiratory flow rate. For example, at a resting respiratory flow rate of 150 ml/s, ~95% of the inspired Cl_2 and 80–90% of the inspired O_3 was absorbed in the N/O compartment and <1% of the inspired Cl_2 or O_3 was absorbed in the RA. At a higher respiratory flow rate of 1,000 ml/s, the Cl_2 dose distribution changed only slightly: 90 and 85% of the inspired Cl_2 was absorbed in the NS and OR compartments, respectively, and <1% of the inspired Cl_2 was absorbed in the RA. The dose distribution of O_3, however, changed substantially: only 45 and 25% of the inspired O_3 was absorbed in the NS and OR compartments, respectively, and 5–10% of the inspired O_3 was absorbed in the RA.

Mass transfer coefficients. Table 2 summarizes the *Ka* values that were calculated from the individual regression of each subject's Λ-V_P distribution. At all three respiratory flow rates, the values of *Ka* were significantly higher for Cl_2 than for O_3 in the NS and OR compartments ($P < 0.04$), but not in the PH and LA compartments ($P > 0.1$). Furthermore, the values of *Ka* for O_3 were always significantly higher in the NS compartment than in the OR compartment ($P < 0.02$) but were similar in the PH compartment during both modes of breathing ($P > 0.2$). In contrast, the *Ka* values for Cl_2 were larger in the NS compartment than in the OR compartment at the higher respiratory flow rates ($P < 0.04$), but not at the lowest respiratory flow ($P = 0.5$). Because of extensive absorption of Cl_2 and O_3 in

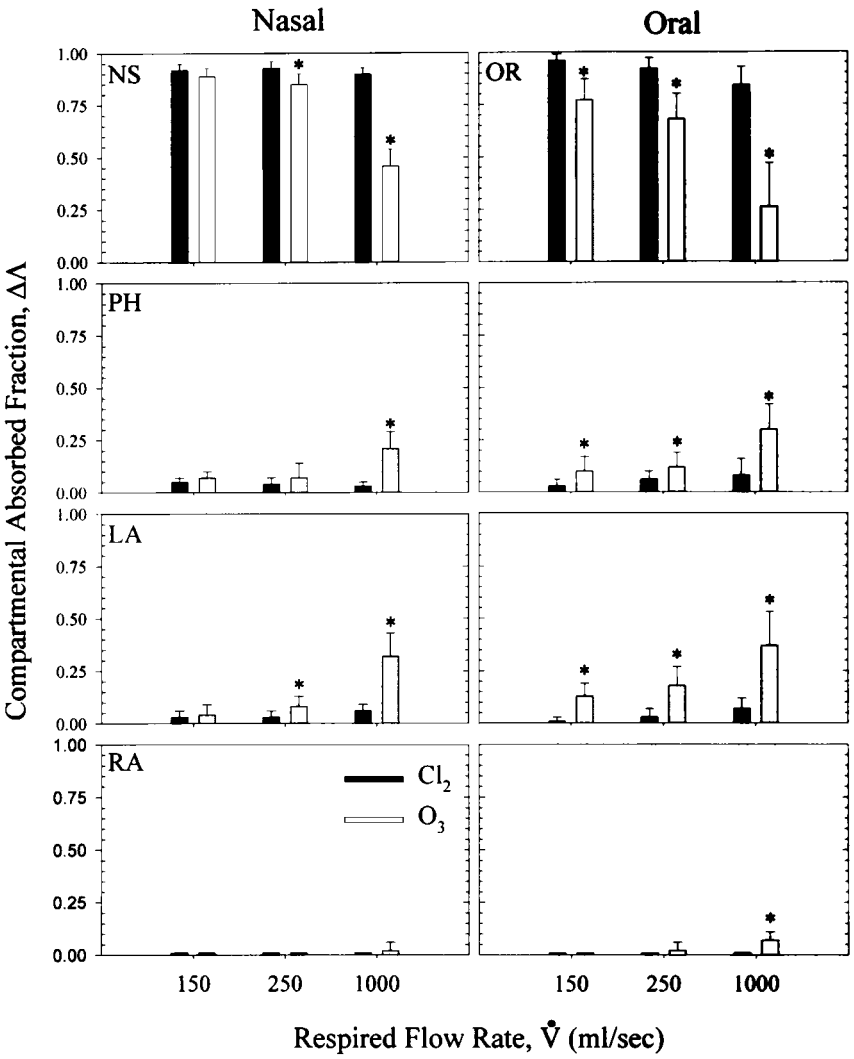

Fig. 3. Compartmental absorption pooled for 10 subjects. Histogram units represent mean $\Delta\Lambda$ for nasal (NS), oral (OR), pharyngeal (PH), lower airway (LA), and respiratory air space (RA) compartments. Vertical bars represent SD of $\Delta\Lambda$ among subjects. * Significant difference between $\Delta\Lambda_{Cl_2}$ and $\Delta\Lambda_{O_3}$ ($P < 0.05$).

the proximal compartments, there was a paucity of Λ-V_P data in the PH and LA compartments, resulting in large uncertainties in the *Ka* values. In some subjects, there were insufficient data to even compute *Ka* in the PH and LA compartments.

Table 3 summarizes the values of the gas phase absorption parameter ($k_g a/\dot{V}$) and the mucus phase absorption parameter ($k_{ti}a/\lambda$) that were estimated by regression of each subject's *Ka* values in the NS, OR, and PH compartments according to *Eq. 8*. Because of extensive absorption in the NS and OR compartments, however, the *Ka* data were only sufficient to compute absorption parameters for the PH compartment in one subject during nasal breathing and two subjects during oral breathing. Theoretically, $k_g a/\dot{V}$ is essentially the same for Cl_2 and O_3, but $k_{ti}a/\lambda$ can have separate values for the two gases. In fact, the value of $(\lambda/k_{ti}a)_{Cl_2}$ was so small that the tissue phase did not limit the rate of Cl_2 absorption. On the other hand, $(k_{ti}a/\lambda)_{O_3}$ did have a significant effect on O_3 absorption. As suggested by the standard deviations in Table 3, there was no significant difference between $k_g a/\dot{V}$ values in the NS and OR compartments ($P = 0.9$), but the value of $(k_{ti}a/\lambda)_{O_3}$ was larger in the NS compartment than in the OR compartment ($P = 0.09$).

DISCUSSION

The primary objective of this research was to determine how the physical-chemical properties of Cl_2 and O_3 affect their uptake distributions in the intact respiratory tract. To be absorbed into the epithelial lining fluid (ELF), both gases must overcome the in-series diffusion resistances of the respired gas and adjacent liquid film (*Eq. 2*). Because both gases have similar diffusion coefficients in respired air, their gas phase diffusion resistances should be similar, an expectation that is illustrated by the parallelism of the lines in the $(1/Ka)$-$(1/\dot{V})$ correlation (Fig. 1). It follows that differences between the absorption rates of these two gases are due to their interactions with the ELF.

The physical solubilities of Cl_2 and O_3 in ELF are low, but Cl_2 reacts with water to form hypochlorous and hydrochloride acids, whereas O_3 irreversibly oxidizes biochemical substrates such as albumin, fatty acids, urate, and ascorbate. Because of the abundance of

Table 2. *Compartmental values of the overall absorption parameters*

Flow, ml/s	$(Ka)_{N/O}$, s^{-1}	$(Ka)_{PH}$, s^{-1}	$(Ka)_{LA}$, s^{-1}	V_{P0}, ml
		Cl_2-nasal		
150	3.4 ± 0.4	1.2 ± 1.2 (8)	0.6 ± 0.1 (2)	5.2 ± 5.2
250	6.2 ± 0.8	1.0 ± 1.0 (8)		7.7 ± 2.6
1,000	25.3 ± 5.5	6.8 ± 7.7 (9)		15.6 ± 5.4
		Cl_2-oral		
150	3.2 ± 0.9	0.3 ± 0.5 (6)		−1.6 ± 9.7
250	4.8 ± 1.3	1.6 ± 1.4 (7)		0.9 ± 5.7
1,000	18.8 ± 5.3	9.2 ± 9.8	8.5 ± 1.7 (3)	16.8 ± 4.0
		O_3-nasal		
150	2.9 ± 0.4	1.9 ± 1.3 (7)	2.1 ± 0 (1)	5.7 ± 2.9
250	4.9 ± 1.1	2.0 ± 2.5		12.2 ± 3.1
1,000	6.2 ± 1.4	12.0 ± 5.7	16.1 ± 4.9	13.8 ± 9.5
		O_3-oral		
150	1.6 ± 0.5	2.2 ± 0.9	1.0 ± 1.0 (3)	3.5 ± 4.9
250	2.6 ± 0.4	3.2 ± 2.3	2.3 ± 0.8 (8)	14.3 ± 4.4
1,000	4.0 ± 2.5	15.3 ± 7.0	10.7 ± 4.9	46.6 ± 22.6

Values are means ± SD of Ka and V_{P0} computed by averaging individual values from all 10 subjects unless fewer subjects are noted in parentheses. $(Ka)_{N/O}$, absorption parameter in nasal cavity and nasopharynx during nasal breathing or in oral cavity and oropharynx during oral breathing; $(Ka)_{PH}$ and $(Ka)_{LA}$, absorption parameters in PH and LA, respectively; V_{P0}, intercept of regression (*Eq. 1*).

water in ELF, the Cl_2 hydrolysis reaction occurs rapidly and with such a large equilibrium constant that the concentration of Cl_2 in the form of the acid ions is ~120,000 times the concentration of molecular Cl_2 (12). In other words, hydrolysis suppresses the backpressure of Cl_2 everywhere in ELF and thereby minimizes the diffusion resistance of Cl_2 in ELF. The concentrations of oxidizable substrates in ELF are low, however, so the reaction rate of O_3 is not sufficiently fast to eliminate the backpressure of O_3 as an impediment to absorption. One would therefore expect that the diffusion resistance of Cl_2 in ELF would be smaller than that of O_3. This is exemplified by the intercepts of the $(1/Ka)$-$(1/\dot{V})$ correlation (Fig. 1).

Because the liquid phase diffusion resistance of Cl_2 is so small, the absorption rate of Cl_2 is generally limited by gas phase diffusion, which is proportional to respiratory flow rate. This is exactly counterbalanced by the inverse dependence of bolus residence time on respiratory flow rate, explaining why the Λ-V_P distribution for Cl_2 is relatively insensitive to respiratory flow (Fig. 2). On the other hand, the O_3 absorption rate is sensitive to diffusion through ELF, which is independent of respiratory flow rate. Therefore, a progressive reduction of absorption occurs in the proximal airways as increases in respiratory flow shorten the residence time of a bolus. This is the basis of the progressive distal shift of the O_3 distribution that occurs as respiratory flow rate increases.

At the lowest nasal respiratory flow of 150 ml/min, the gas phase diffusion resistances of Cl_2 and O_3 dominate their liquid phase resistances, so that the Λ-V_P distributions for the two gases are similar (Fig. 2). During an oral flow of 150 ml/min, however, a significant resistance of O_3 diffusion through ELF causes a distal shift of the O_3 distribution relative to the corresponding Cl_2 distribution. Because the saliva in the mouth probably lacks much of the antioxidant capacity of nasal mucus, it is not surprising that the diffusion resistance of O_3 is more important in the mouth than in the nose. The hydrolysis of Cl_2, on the other hand, should suppress the diffusion resistance of the liquid film in the nose and the mouth.

The specific values of the liquid phase resistance $(\lambda/k_{ti}a)$ for O_3 were 0.042 s in the nasal compartment and 0.18 s in the oral compartment, whereas $\lambda/k_{ti}a$ values estimated for Cl_2 were not significantly different from zero. Because of this, the gas phase resistance of Cl_2 accounted for 100% of the overall diffusion resistance in the nasal and oral compartments at all respiratory flow rates. On the other hand, the gas phase resistance of O_3 at respiratory flow rates of 150, 250, and 1,000 ml/s made contributions to the overall nasal diffusion resistance of 86, 79, and 49%, respectively, and contributions to the overall oral diffusion resistance of 64, 51, and 21%, respectively.

Table 3. *Compartmental values of the individual absorption parameters*

	$(k_g a/\dot{V})_{N/O}$, $liters^{-1}$		$(k_g a/\dot{V})_{PH}$, $liters^{-1}$		$(k_{ti}a/\lambda)_{N/O}$, s^{-1}		$(k_{ti}a/\lambda)_{PH}$, s^{-1}	
Gender	Nasal	Oral	Nasal	Oral	Nasal	Oral	Nasal	Oral
male (m)	22 ± 1	27 ± 3			13 ± 3	3.3 ± 0.5		
m	25 ± 4	31 ± 9	11 ± 1	11 ± 2	13 ± 7	2.9 ± 2.0	35 ± 38	8 ± 7
m	27 ± 3	28 ± 2		16 ± 10	10 ± 3	4.9 ± 1.7		11 ± 30
m	23 ± 1	15 ± 1			10 ± 2	5.1 ± 0.6		
m	26 ± 5	13 ± 1			16 ± 11	4.4 ± 0.5		
f	24 ± 3	13 ± 5			8 ± 3	12.3 ± 3.7		
female (f)	28 ± 3	19 ± 4			28 ± 25	4.7 ± 2.0		
f	24 ± 3	16 ± 1			17 ± 8	7.8 ± 1.6		
f	26 ± 4	23 ± 4			59 ± 123	4.8 ± 1.2		
f	22 ± 4	22 ± 1			64 ± 159	5.8 ± 0.5		
Mean ± SD	25 ± 2	21 ± 7	11	14 ± 4	24 ± 21	5.6 ± 2.7	35	9.5 ± 2.5

Values are means ± SD of absorption parameters computed by averaging individual values from all subjects. $(k_g a/\dot{V})_{N/O}$, gas phase absorption parameter for Cl_2 and O_3 in nasal cavity and nasopharynx during nasal breathing or in oral cavity and oropharynx during oral breathing; $(k_g a/\dot{V})_{PH}$, gas phase absorption parameter for Cl_2 and O_3 in PH; $(k_{ti}a/\lambda)_{N/O}$ and $(k_{ti}a/\lambda)_{PH}$, corresponding tissue absorption parameters that apply to O_3 only.

Although *Ka* values in the nose and mouth were generally larger for Cl_2 than for O_3, most paired comparisons of *Ka* values in the PH and LA compartments showed a lack of significant differences between Cl_2 and O_3. A post hoc power analysis indicated, however, that the probability of a type II error (i.e., falsely concluding that the values of *Ka* for Cl_2 and O_3 were similar) was ~0.75. Reduction of this probability to an acceptable level of 0.2 would require testing approximately twice as many subjects or improving the precision of the test breath concentration data, possibly by increasing the peak inhaled bolus concentration.

A substantial dose of O_3 was absorbed in the LA compartment under all experimental conditions and in the RA compartment during oral breathing at the highest respiratory flow rate of 1,000 ml/s (Fig. 3). This suggests that an increase in respiratory flow coupled with a switch from nasal to oral breathing, as normally occurs during exercise, is likely to cause a distal shift in the O_3 dose distribution, which increases the likelihood of damage to alveolar and bronchiolar tissues. In contrast, inspired Cl_2 was primarily absorbed in the NS and OR compartments. Even during oral breathing at a respiratory flow of 1,000 ml/s, >85% of the inspired Cl_2 was still absorbed in the OR compartment compared with only 25% of the inspired O_3 (Fig. 3). Because this result was consistent for all 10 subjects, it is likely that Cl_2-induced tissue damage is localized in the upper airways of the human respiratory tract, irrespective of the mode of breathing or respiratory flow rate.

The measurements of O_3 bolus inhalation in this study are consistent with the results of previous studies that used healthy nonsmokers. Hu et al. (8) showed that Λ was ~0.50 at a V_P of 50 ml and 0.90 at a V_P of 170 ml during oral breathing at 150 ml/s. When the oral flow was increased to 1,000 ml/s, Λ decreased to ~0.10 at a V_P of 50 ml and to 0.75 at a V_P of 170 ml. In the present study the corresponding values of Λ were ~0.60 and 0.95 during oral breathing at 150 ml/s and 0.10 and 0.90 during oral breathing at 1,000 ml/s (Fig. 2). Therefore, the Λ values obtained during oral breathing of O_3 in this study were slightly higher than those reported previously. This previous study did not include female subjects, who are known to exhibit higher Λ values than men during oral breathing (3). During nasal breathing at a respired flow rate of 250 ml/s, Kabel et al. (9) reported Λ of ~0.70 at a V_P of 50 ml and 0.90 at a V_P of 170 ml. In this study, corresponding values of Λ were ~0.65 and 0.95. Thus the Λ values obtained during nasal quiet breathing were quite similar in the present and the previous study.

Previous studies have shown that Cl_2 and O_3 uptake rates during quiet breathing are related to airway geometry because of its effect on the gas phase diffusion resistance (3, 12). To further explore this phenomenon in the present study, *Eq. 7* was applied to the N/O compartment. By writing *a* in an explicit manner, *Eq. 7* becomes

$$k_g a/\dot{V} = (m/V)(S/A) \qquad (9)$$

where V, *S*, and *A* are the airway volume, surface area, and average cross-sectional area, respectively. If the geometric shape of an airway was the same in everyone, then the *S*/*A* ratio would be a constant from subject to subject and $k_g a/\dot{V}$ would be inversely proportional to the airway volume. To test this possibility, a weighted log-log regression of the individual subject's values of $k_g a/V$ to the corresponding values of V was performed in the NS as well as in the OR compartment. Weights were computed as the squared reciprocal of the standard error of each value of $k_g a/V$.

The results of the two regressions were as follows (Fig. 4)

$$(k_g a/\dot{V})_{OR} = 0.44(V_{OR}^{-0.79\pm0.09}) \qquad (10)$$

and

$$(k_g a/\dot{V})_{NS} = 0.22(V_{NS}^{-0.58\pm0.16}) \qquad (11)$$

where the standard error is shown for the regressed value of the exponent. For the OR compartment described by *Eq. 10*, variations in $(k_g a/V)_{OR}$ were almost completely predicted by variations in V_{OR} ($r^2 = 0.89$), and the exponent on airway volume was not much different from the expected value of -1.0 ($P = 0.043$). This indicates that everyone's mouth had a similar shape, as was also suggested by the strong correlation between V_{OR} and A_{OR} ($r^2 = 0.85$). For the NS compart-

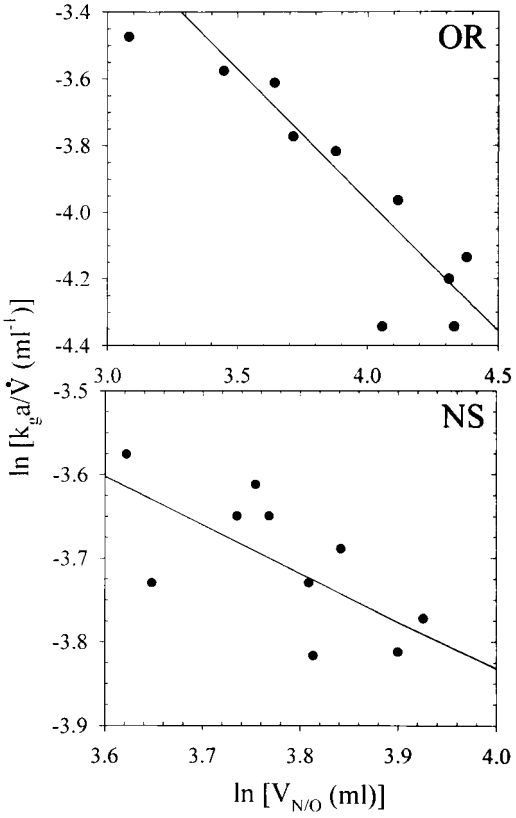

Fig. 4. Influence of volume in nasal or oral cavity ($V_{N/O}$) on gas phase mass transfer parameter ($k_g a/\dot{V}$). Each data point represents value of $k_g a/\dot{V}$ in mouth (OR) or nose (NS) of an individual subject. Solid lines, weighted least-squares regression of $\ln(k_g a/\dot{V})$ against $\ln(V_{OR})$ for oral data and against $\ln(V_{NS})$ for nasal data.

ment described by *Eq. 11*, variations in $(k_g a/\dot{V})_{NS}$ were not as well predicted by variations in V_{NS} ($r^2 = 0.61$), and the exponent on V_{NS} deviated from -1.0 ($P = 0.033$) by a greater amount. These results suggest that the shape of the nasal compartment was not constant among the 10 subjects. This conclusion is also consistent with the fact that V_{NS} was not correlated with A_{NS} ($r^2 = 0.00$).

At the highest respiratory flow employed in this study, the spatial resolution of the bolus inhalation method was limited. During each test breath, a pulse of Cl_2-air (or O_3-air) was injected into the inhaled airstream by using a miniature solenoid valve that was opened for 0.1 s. At the lowest airflow of 150 ml/s, the Cl_2 pulse formed an inhaled bolus by mixing with the 15 ml of air that passed the injection point during 0.1 s. At the highest airflow of 1,000 ml/s, the Cl_2 pulse mixed with 100 ml of air to form the inhaled bolus. In other words, the volume of the inhaled Cl_2-air (or O_3-air) bolus ranged from 15 ml at 150 ml/s, which was smaller than the smallest compartmental volume, to 100 ml at 1,000 ml/s, which was somewhat larger than the largest compartmental volume (Table 1). In addition to dispersive mixing of the inhaled bolus, dispersion occurred as the bolus was convected within the respiratory system (12). This further compromised the spatial resolution of the absorption data.

Summary. The longitudinal distribution of Cl_2 and O_3 absorption was measured by the bolus inhalation method in 10 subjects during nasal and oral breathing at flow rates of 150, 250, and 1,000 ml/s. Irrespective of the mode of breathing and respiratory flow rate, >95% of the inspired Cl_2 was absorbed in the upper airways, whereas the dose delivered to the lower airways was <5%. In contrast, the dose distribution of O_3 was relatively sensitive to the mode of breathing as well as to respiratory flow rate. As respiratory flow increased, the O_3 dose delivered to the upper airways ranged from 95 to 50%, whereas the dose delivered to the LA ranged from 0 to 35%. These differences between Cl_2 and O_3 dosimetry were attributed to the greater tissue phase resistance of O_3 than of Cl_2. During quiet oral breathing, tissue phase diffusion resistance accounted for ~50% of the overall absorption resistance of O_3 but for virtually none of the overall absorption resistance of Cl_2. The lack of a tissue phase resistance for Cl_2 probably resulted from its rapid hydrolysis in the airway mucosa. The gas phase resistances of Cl_2 and O_3 were similar and were related in an inverse manner to the volumes of the oral and nasal cavities.

The authors are grateful to S. Arnold, R. Bascom, and A. Ben-Jebria for insightful suggestions.

This work was supported in part by the Chlorine Institute through a subcontract with the Chemical Industry Institute of Toxicology and by National Institute of Environmental Health Sciences Research Grant ES-06075. Clinical support was provided by the General Clinical Research Center through funding by National Institutes of Health Grant M01 RR-10732.

Address for reprint requests and other correspondence: J. S. Ultman, Dept. of Chemical Engineering, Penn State University, 106 Fenske Lab, University Park, PA 16802 (E-mail: JSU@PSU.EDU).

Received 23 November 1998; accepted in final form 26 July 1999.

REFERENCES

1. **American Conference of Government Industrial Hygenists.** *1996–1997 Threshold Limit Values for Chemical Substances, and Physical Agents and Biological Exposure Indices.* Cincinnati, OH: American Conference of Government Industrial Hygenists, 1996.
2. **Barry, B. E., F. J. Miller, and J. D. Crapo.** Effects of inhalation of 0.12 and 0.25 parts per million ozone on the proximal alveolar region of juvenile and adult rats. *Lab. Invest.* 53: 692–704, 1985.
3. **Bush, M. L., P. T. Asplund, K. A. Miles, A. Ben-Jebria, and J. S. Ultman.** Longitudinal distribution of ozone absorption in the lung: gender differences and intersubject variability. *J. Appl. Physiol.* 81: 1651–1657, 1996.
4. **Castleman, W. L., W. S. Tyler, and D. L. Dungworth.** Lesions in respiratory bronchioles and conducting airways of monkeys exposed to ambient levels of ozone. *Exp. Mol. Pathol.* 26: 384–400, 1977.
5. **Gerrity, T. R., F. Biscardi, A. Strong, A. R. Garlington, J. S. Brown, and P. A. Bromberg.** Bronchoscopic determination of ozone uptake in humans. *J. Appl. Physiol.* 79: 852–860, 1995.
6. **Gerrity, T. R., R. A. Weaver, J. Berntsen, D. E. House, J. J. O'Neil.** Extrathoracic and intrathoracic removal of ozone in tidal-breathing humans. *J. Appl. Physiol.* 95: 393–400, 1988.
7. **Hu, S. C., A. Ben-Jebria, and J. S. Ultman.** Longitudinal distribution of ozone absorption in the lung: quiet respiration in healthy subjects. *J. Appl. Physiol.* 73: 1655–1661, 1992.
8. **Hu, S. C., A. Ben-Jebria, and J. S. Ultman.** Longitudinal distribution of ozone absorption in the lung: effects of respiratory flow. *J. Appl. Physiol.* 77: 574–583, 1994.
9. **Kabel, J. R., A. Ben-Jebria, and J. S. Ultman.** Longitudinal distribution of ozone absorption in the lung: comparison of nasal and oral quiet breathing. *J. Appl. Physiol.* 77: 2584–2592, 1994.
10. **Klonne, D. R., C. E. Ulrich, M. G. Riley, T. E Hamm, Jr., K. T. Morgan, and C. S. Barrow.** One-year inhalation toxicity study of chlorine in rhesus monkeys (*Macaca mulatta*). *Fundam. Appl. Toxicol.* 9: 557–572, 1987.
11. **McDonnell, W. F., D. H. Horstman, M. J. Hazucha, E. Seal, E. D. Haak, S. A. Salaam, and D. E. House.** Pulmonary effects of ozone exposure during exercise: dose-response characteristics. *J. Appl. Physiol.* 54: 1345–1352, 1983.
12. **Nodelman, V., and J. S. Ultman.** Longitudinal distribution of chlorine absorption in the human airways: comparison of nasal and oral quiet breathing. *J. Appl. Physiol.* 86: 1984–1993, 1999.
13. **Nuckols, M. L.** *Heat and Water Vapor Transfer in the Human Respiratory System at Hyperbaric Conditions* (Doctoral dissertation). Durham, NC: Duke University, 1981.
14. **Rotman, H. H., M. J. Fliegelman, T. Moore, R. G. Smith, D. M. Anglen, C. J. Kowalski, and J. G. Weg.** Effects of low concentrations of chlorine on pulmonary function in humans. *J. Appl. Physiol.* 54: 1120–1124, 1983.
15. **Treybal, R. E.** *Mass-Transfer Operations* (3rd ed.). New York: McGraw-Hill, 1980, chapt. 2, p. 31–34; chapt. 3, p. 70–77; chapt. 5, p. 109–111.
16. **Wolf, D. C., K. T. Morgan, E. A. Gross, C. Barrow, O. R. Moss, R. A. James, and J. A. Popp.** Two-year inhalation exposure of female and male B6C3F1 mice and F344 rats to chlorine gas induces lesions confined to the nose. *Fundam. Appl. Toxicol.* 24: 111–131, 1995.